M. HAUER[1]
D.J. FUNK[2]
T. LIPPERT[1],✉
A. WOKAUN[1]

Laser induced decomposition of a designed and a commercial polymer studied by ns-interferometry and shadowgraphy

[1] General Energy Research, Paul Scherrer Institut, 5232 Villigen PSI, Switzerland
[2] DX-2, MS C920, Los Alamos National Laboratory, Los Alamos, NM 87545, USA

ABSTRACT Commercially available polymers often exhibit quite poor laser ablation properties for irradiation wavelengths around 248 nm. At these wavelengths, the absorption is due to photostable aromatic groups. Photolabile triazene polymers were developed to compare the influence of a photolabile group on the laser ablation process. The photochemically active triazene group has a strong absorption band at 332 nm, whereas the second absorption maximum at 220 nm is due to the photostable aromatic group. By irradiating at 308 nm and 193 nm, the influence of the photochemically active group on the ablation process can be studied. The etching of the triazene polymer starts and ends with the laser pulse. No surface swelling, which is assigned to photothermal ablation, is detected for fluences above the threshold of ablation. The expansion of the laser ablation induced shockwave was measured for the photolabile triazene polymer and the photostable polyimide. The speed of the shockwave increases with fluence and is higher for irradiation with 193 nm than with 308 nm. A shockwave with equal or higher velocity is observed for the triazene polymer compared with polyimide.

PACS 52.38.Mf; 42.87.Bg; 71.20.Rv

1 Introduction

Since 1982, when laser ablation was first reported [1, 2], it has been studied using a variety of techniques, but the ablation mechanism still remains controversial. It has been emphasized that a better understanding of the temporal behavior of the ablation process is fundamental to an understanding of the physical chemistry of this phenomenon. Many different approaches, such as time resolved absorption [3] and emission spectroscopy [4], time resolved Raman spectroscopy [5, 6], time resolved infrared spectroscopy [7, 8] and time resolved quadrupole mass spectroscopy [9–12] have been used to obtain a better understanding of the ablation process.

In this study, the laser ablation process for a photolabile triazene polymer, which exhibits superior laser ablation characteristics (sharp ablation edges, no debris, low threshold fluence, and high etch rates at low fluences [13–15]),

✉ Fax: +41-56/310-4412, E-mail: thomas.lippert@psi.ch

is studied using ns-interferometry. The polymer has an absorption maximum around 200 nm, which is due to the photostable aromatic system. A second absorption maximum around 332 nm is due to the photolabile triazene group. Both absorption maxima have similar absorption coefficients ($\approx 100\,000\,\text{cm}^{-1}$). The influence of the different chromophores on the surface morphology changes during the ablation process can be studied by irradiation with 308 and 193 nm.

Nanosecond-surface interference measurements have shown that time resolved surface profiling of the ablated area can give valuable information about the ablation process. It has been demonstrated that some polymers exhibit a pronounced swelling before ablation is observed [16, 17], whereas the ablation process of another polymer starts and ends with the laser pulse [18]. The surface swelling has been attributed to a photothermal process, while the absence of this swelling has been interpreted as an indication of a photochemical process.

Complementary information can be obtained by shadowgraphy, where the laser ablation induced shockwave is analyzed. It has been shown, that the ejection of solid material can be detected by shadowgraphy [3, 16, 19] and that in some cases, the expansion of the shockwave cannot be fully explained by the deposited laser energy. In this case, it is necessary to include the decomposition enthalpy of the polymer in the shockwave analysis [20]. The shadowgraphy measurements were also performed with polyimide, to have a standard polymer that has similar absorption coefficient at 308 nm as a reference. This allows the direct comparison of the photolabile triazene polymer and the photostable polyimide.

2 Experimental

The triazene polymer (shown in Fig. 1) was prepared by a previously described method [21]. The 1- to 2 µm thick polymer films were spin coated from a chlorobenzene solution (10% polymer) and dried at 40 °C for 24 h. The polyimide film (75 µm thick, Kapton[TM]HN) was obtained from DuPont. All measurements were performed under ambient pressure at room temperature.

The experimental setup for the surface interference measurements is a pump–probe setup. A Compex 205 XeCl excimer laser from Lambda Physik (FWHM of 30 ns) is applied as the pump laser (308 nm irradiation), while for the irradi-
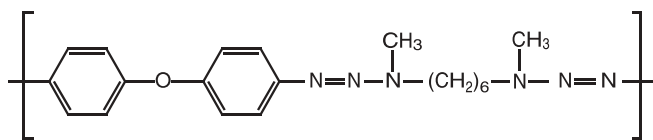
FIGURE 1   Chemical structure of the triazene polymer

ation at 193 nm, a LPX 301i ArF excimer laser (Lambda Physik, FWHM of 25 ns) is used. The probe laser (2nd harmonic of a Brillant Bω Nd:YAG laser from Quantel with a FWHM of 5 ns) is used in a Michelson interferometric setup. The probe beam is divided by a beamsplitter (50 : 50) and one beam is reflected by a wedged substrate (allowing the reflection from the air/quartz interface to be selected). The other beam passes from the rear side of the sample through the wedged substrate and polymer and is reflected at the polymer/air interface. This has the advantage that the ejected material does not disturb the probe beam. Both beams are recombined in the beamsplitter and create an interference fringe pattern. A fringe shift is obtained for changes of film thickness or refractive index of the polymer, which will alter the effective path length of the probe beam through the polymer.

The refractive index of the polymer is obtained by comparing the final fringe shift with the ablation depth measured with a surface profilometer (Dektak 8000 from Sloan Technologies). The fringe shift is proportional to the surface displacement, assuming that the ablation process does not affect the refractive index. Both lasers are timed with a delay generator (DG 535 from SRS) and the surface fringes are recorded with a CCD camera. In the following, the time origin, $t = 0$ ns, was chosen as the time where the laser pulse reached 1% of its maximum intensity. The surface profile at a specific time can be extracted by evaluating (described later) the fringe shifts.

For the shadowgraphy experiments, the optical pathway of the probe laser is modified to a Mach–Zehnder interferometer setup [22]. One beam of the interferometer passes parallel to the surface of the polymer, through the ablation plume, while the other beam is unaffected by the ablation process. Both beams are recombined in a second beamsplitter, where the fringe pattern is created. The compressed (i.e. ablation products and air) gases in the shockwave of the ablation have a higher refractive index than the ambient atmosphere. A fringe shift results, which is proportional to the changes of the refractive index and path length of the probe beam through the ablation plume.

The evaluation of the fringe shifts was done according to a procedure described elsewhere [23, 24]. Briefly, during both experiments, a picture is recorded before and during/after the pump. These two pictures are transformed using a 2D fast Fourier procedure (2D FFT). The images can be reduced to the fringe information by selecting one specific peak from the fringes in the 2D FFT images and filtering all other peaks. The images were then inverse Fourier transformed into the complex space. The phase difference Δp between the reference and the measurement picture is then proportional to the fringe shift Δd, with λ = wavelength and n_D = refractive index, i.e.,

$$\Delta p(\Delta d) = 4\pi \frac{\Delta d n_D}{\lambda}. \tag{1}$$

The dynamic range of the phases is limited to 2π. A phase jump will result if the phase shift between both pictures exceeds this limited range. It is very important during the data analysis to include these phase jumps, otherwise the wrong ablation depths are obtained.

The ablation depth was measured from the phase shift images taken from the surface interference setup. The phase shift of the non-irradiated area changes from measurement to measurement due to instabilities of the interference pattern. This causes a varying constant offset from measurement to measurement. Therefore, the difference between the phase shifts of the irradiated and non-irradiated areas was analyzed. By taking the wavelength of the probe beam, the refractive index of the polymer, and the phase jumps into account in the analysis procedure, the surface displacement at a specific time during or after the laser pulse can be determined.

The shadowgraphy setup was applied to measure the expansion of the shockwave from the phase shift images. Measuring the distance between the shockwave front and the polymer surface allows the propagation speed of the shockwave to be determined.

3   Results and discussion

3.1   *ns- Interferometry*

The surface displacement of the triazene polymer after irradiation with 308 nm for different fluences is shown in Fig. 2. The data taken at 10 mJ cm^{-2}, which is below the ablation threshold of the triazene polymer ($F_{th} = 27$ mJ cm^{-2} at 308 nm, measured with multiple laser pulses [18]) reveal a slight surface swelling that starts with the laser pulse and disappears after several seconds. No permanent modification of the polymer surface is observed. This is probably due to the decomposition of the photolabile triazene chromophore, which results in the release of nitrogen, which is observed even for very low irradiation intensities (e.g. $\approx$ mW cm^{-2} [18]). The trapped nitrogen causes a transient swelling, until the nitrogen escapes by diffusion.
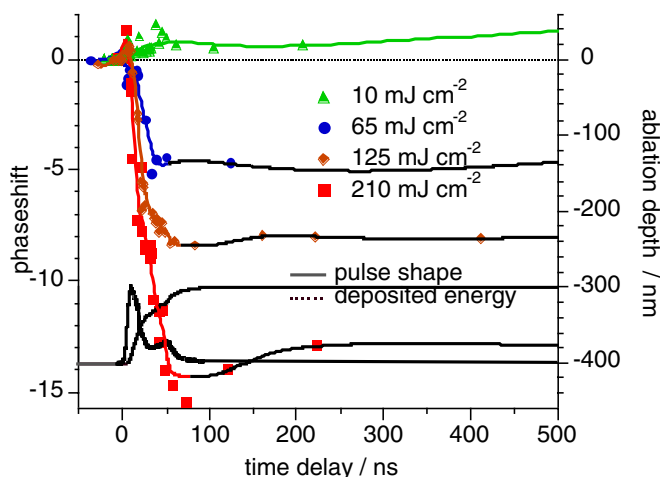

FIGURE 2   Ablation depth of the triazene polymer after irradiation at 308 nm. A *smoothed spline curve* has been added to guide the eye along the data points. In the *lower left* area, the relative intensity and integrated power of the laser pulse is included. The ablation depth was calculated assuming $n_D = 1.44$

At higher fluences, the phase shift starts with the laser pulse and a very short (10 ns) positive phase shift is observed for fluences of 125 and 210 mJ cm^{-2}. This phase shift may be due to a very dense gas layer, which is created during the initial ablation process. Such a gas layer should have a high refractive index, which will cause a reflection of the probe beam at this gas/air interface. When the gas expands, the refractive index will decrease and the beam will be reflected at the polymer/air interface.

A change of the refractive index of the polymer will also cause a fringe shift and might explain the temporary positive phase shift. Reflectivity measurements of the polymer during and after the laser (by comparing the amplitude of the reference and measurement pictures) reveal that the reflectivity decreases with the laser pulse and recovers after 50 ns. These reflectivity changes may be due to changes of the refractive index or a temporary surface roughening. This indicates that the optical properties of the polymer change during the ablation process. Whether this change or the formation of the expanding gas is responsible for the fringe shift remains unclear at the moment.

The transient increase of the phase shift is followed by a permanent decrease of the phase shift. This phase shift corresponds to ablation of the polymer in the irradiated area. The decrease of the phase shift ends with the end of the laser pulse, indicating a photochemical ablation process.

The surface interference measurements after 193 nm irradiation reveal a very similar behavior. At the lowest applied fluence of 10 mJ cm^{-2} (around the ablation threshold of 12 mJ cm^{-2}), a temporary phase shift corresponding to an ablation of 20 nm is observed. After several seconds, this phase shift disappears almost completely, which can be explained by changes of the optical refractive index.

At the higher fluences, a fast transient positive phase shift, similar to that observed for 308 nm irradiation, is observed. This positive phase shift is followed by a negative phase shift, which ends with the laser pulse. Both types of phase shift have already been discussed for 308 nm irradiation.

The ablation process starts and ends at both wavelengths with the laser pulse. A positive phase shift can only be observed for a very short time period ($\approx$ 10 ns). This cannot be explained by a thermal swelling of the polymer, which has been observed for other polymers on a much longer time scale ($\approx \mu$s) [8]. The absence of thermal swelling and the observation that the end of the ablation process corresponds with the end of the laser pulse are strong indications that, at both wavelengths, a photochemical ablation mechanism is at least partly responsible for the ablation process.

3.2 *Shadowgraphy*

The shockwave starts initially with a planar expansion. This expansion changes to a stretched hemispherical expansion (the expansion perpendicular to the surface is faster than that parallel to the surface). Only the expansion perpendicular to the surface is analyzed in more detail below.

Figure 3 shows the propagation of the shockwave created by irradiation of the triazene polymer and polyimide in air at 193 nm. Polyimide was used as the reference polymer, to compare a photostable and photolabile polymer. The
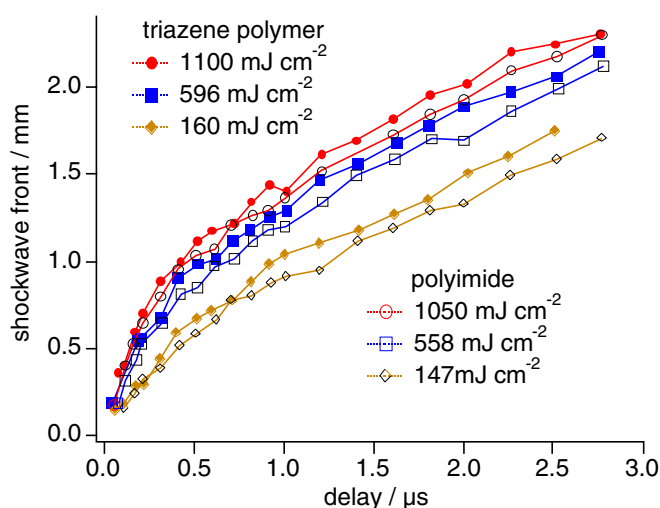

FIGURE 3   The propagation of the shockwave after irradiation of the triazene polymer at 193 nm for different fluences (measured perpendicular to the surface of the polymer). Polyimide was included as a reference polymer to quantify the influence of the polymer properties on the ablation process and shockwave propagation

velocities of shockwaves from the triazene polymer are always faster than those observed for polyimide. This is due to the higher ablation rates and greater fragmentation of the triazene polymer (see Table 1). The higher ablation rates and the higher fragmentation will increase the amount of gaseous ablation products (and the pressure in the shock wave), resulting in shockwaves with higher velocities.

The propagation of the shockwave created from the triazene polymer is faster for irradiation with 193 nm light than for 308 nm at all applied fluences (shown in Fig. 4). At 308 nm, the triazene group of the polymer absorbs the laser light. The photon energy at this wavelength is quite low (4.02 eV), resulting mainly in the decomposition of the triazene group. This will result in large molecular fragments, e.g. diphenylether fragments (168 amu) [11]. The 193 nm photons are absorbed by the aromatic system in the triazene polymer. These photons have a higher energy (6.4 eV) and are therefore able to break most bonds in the polymer (including the C=C bonds of the aromatic system). This results in more and smaller gaseous fragments than for 308 nm irradiation.

	Triazene Polymer		Polyimide	
	193 nm	308 nm	193 nm	308 nm
α_{lin} (cm^{-1})	118000	100000	340000[a]	95000[b]
α_{eff} (cm^{-1})	214000	50000	13000	83000[b]
F_{th} (mJ cm^{-2})	12	27	14 − 30[b,c,d]	60[b]
d (nm/pulse) at 150 mJ cm^{-2}	118	358	65[c]	78[c]
d (nm/pulse) at 600 mJ cm^{-2}	183	635	130[e]	353[e]
d (nm/pulse) at 1000 mJ cm^{-2}	207	737	155[e]	564[e]

[a] from Lit. [25]; [b] from Lit. [18]; [c] from Lit. [26]; [d] from Lit [27]; [e] from Lit [28]

TABLE 1   Chemical properties and ablation parameters of the polymers
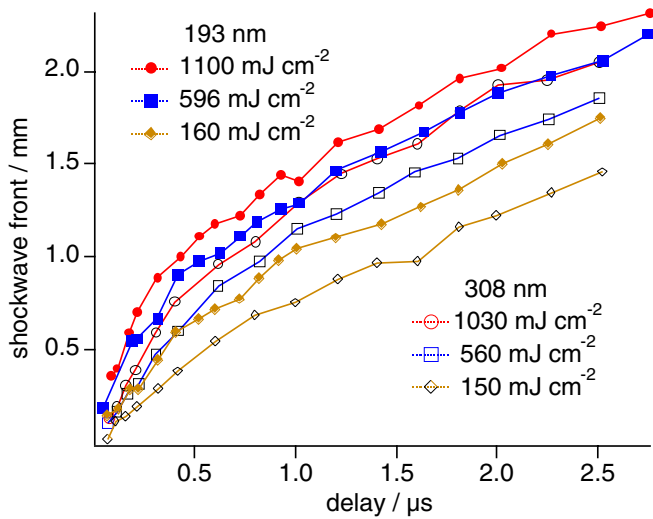
FIGURE 4 The propagation of the shockwave for different fluences after irradiation at 193 and 308 nm (triazene polymer) (measured perpendicular to the polymer surface)

Further indications of this increased fragmentation are the higher effective absorption coefficient α_{eff} and the lower ablation rates (see Table 1). The effective absorption coefficient and the ablation threshold F_{th} are thereby obtained by (2), which relates the single pulse ablation etch rate d to the fluence F [25, 26]:

$$d(F) = \frac{1}{\alpha_{eff}} \ln \frac{F}{F_{th}}. \tag{2}$$

This higher α_{eff} for 193 nm irradiation suggests that the energy is deposited in a thinner layer, probably also resulting in smaller fragments. With 308 nm irradiation, more polymer is ablated, but the extended fragmentation for 193 nm irradiation produces a higher initial velocity of the shockwave.

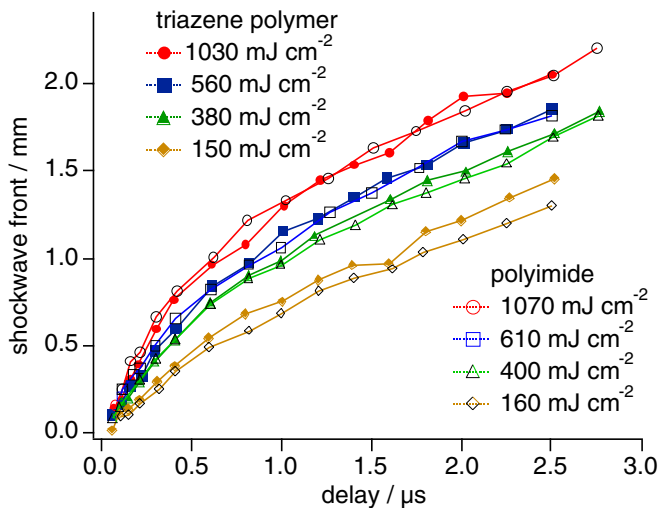Figure 5 shows the propagation of the shockwave of the triazene polymer and polyimide after irradiation at 308 nm.

FIGURE 5 The propagation of the shockwave after irradiation of the triazene polymer at 308 nm for different fluences (measured perpendicular to the surface of the polymer). Polyimide was included as a reference polymer to quantify the influence of the polymer properties on the ablation process and shockwave propagation

Fluence mJ cm^{-2}	Triazene Polymer		Polyimide	
	193 nm	308 nm	193 nm	308 nm
1150	1900	1950	2100	2150
580	1850	1450	1700	1400
150	1300	1000	1100	900

TABLE 2 Summary of the initial shockwave velocities^a (in m s^{-1}) during the first 500 ns
^{a} An important error source is the differences in the timing between the different measurements. The averaging period was not constant, which affects the measured velocities

The shockwaves of both polymers move with the same speed at the two higher fluences. Around 400 mJ cm^{-2}, the initial velocity of the shockwave of the triazene polymer is slightly higher than that observed for polyimide. This difference becomes even more pronounced at the lowest fluence (150 mJ cm^{-2}).

At the lower fluences, the ablation rates are more dependent on the structure of the polymer than at higher fluences, where other processes such as plasma shielding become dominant. This can also be observed when ablation rates of the triazene polymer and the polyimide are compared. (Table 1, at 1 J cm^{-2}, $d_{triazene}/d_{polyimide} = 1.3$ vs. at 150 mJ cm^{-2}, $d_{triazene}/d_{polyimide} = 4.5$). The large difference in the ablation depth results in a difference in the amount of gaseous products. Increasing the amount of gaseous products will increase the speed of the shockwave. The initial speeds of the shockwaves for both polymers at higher fluences are similar for 308 nm irradiation, suggesting that the fragmentation is comparable in these measurements.

All initial shockwaves travel with supersonic speeds, i.e., between 970 and 2080 m s^{-1} (Table 2). The initial speed of the shockwave is related to the amount of gas released during the ablation process. Whether this gas is produced by high ablation rates and larger fragments (low fragmentation of the polymer) or by lower ablation rates and smaller fragments (high fragmentation) seems to be of minor importance. The shockwave velocities after 2 µs are still supersonic and vary between 400 and 500 m s^{-1}. A possible explanation is the volume increase during the expansion of the shockwave. The volume of a hemisphere increases with the cube of the radius. The pressure within the shockwave will decrease at the same time. At some given time, the pressure differences due to the different amounts of gas will have only a minor effect on the velocity of the shockwaves.

4   Conclusion

Nanosecond-interferometry shows that the ablation process of the triazene polymer starts and ends with the laser pulse. Initially, a small positive phase shift is observed. This positive phase shift is transient (10 ns) and is followed by a fast negative shift, which is assigned to ablation of the polymer. The positive phase shift is too fast to be due to a thermal (surface) swelling, as observed for other polymers. The transient phase shift can either be attributed to a dense layer of gaseous ablation products or to changes of the refractive index of the polymer during ablation.

Shadowgraphy measurements were used to measure the laser ablation induced shockwave for the photolabile triazene polymer and for polyimide as a photostable reference polymer. The speed of the shockwave increases with laser fluence and is higher for irradiation with 193 nm than with 308 nm. This is attributed to the higher energy of the 193 nm photons, which are able to fragment the polymer more extensively. The shockwaves created by irradiation of the triazene polymer reveal an equal or higher velocity than those observed for polyimide ablation. The triazene polymer is more sensitive to UV photons (especially at 308 nm) than polyimide and higher ablation rates are obtained. The higher ablation rates result in more gaseous products during the ablation process, which produce a faster shockwave.

REFERENCES

1 R. Srinivasan, V. Mayne-Banton: Appl. Phys. Lett. **41**, 576 (1982)
2 Y. Kawamura, K. Toyoda, S. Namba: Appl. Phys. Lett. **40**, 374 (1982)
3 H. Fukumura, E. Takahashi, H. Masuhara: J. Phys. Chem. A **99**, 750 (1995)
4 H. Fujiwara, H. Fukumoto, H. Fukumura, H. Masuhara: Res. Chem. Intermed. **24**, 879 (1998)
5 D.E. Hare, D.D. Dlott: Appl. Phys. Lett. **64**, 715 (1994)
6 D.E. Hare, J. Franken, D.D. Dlott: J. Appl. Phys. **77**, 5950 (1995)
7 T. Lippert, P.O. Stoutland: Appl. Surf. Sci. **109/110**, 43 (1997)
8 T. Lippert, A. Koskelo, P. Stoutland: J. Am. Chem. Soc. **118**, 1551 (1996)
9 T. Lippert, A. Wokaun, S.C. Langford, J.T. Dickinson: Appl. Phys. A **69**, 655 (1999)
10 T. Lippert, S.C. Langford, A. Wokaun, G. Savas, J.T. Dickinson: Appl. Phys. A **89**, 7116 (1999)
11 M. Hauer, J.T. Dickinson, S.C. Langford, T. Lippert, A. Wokaun: Appl. Surf. Sci. **197–198**, 791 (2002)
12 D.J. Krajnovich: J. Phys. Chem. A **101**, 1175 (1996)
13 J. Wei, N. Hoogen, T. Lippert, O. Nuyken, A. Wokaun: J. Phys. Chem. B **105**, 1267 (2001)
14 T. Lippert, C. David, J.T. Dickinson, M. Hauer, U. Kogelschatz, S.C. Langford, O. Nuyken, C. Phipps, J. Robert, A. Wokaun: J. Photochem. Photobiol. A **87**, 145 (2001)
15 T. Lippert, A. Wokaun, J. Stebani, O. Nyken, J. Ihlemann: Angew. Macromol. Chem. **97**, 206 (1993)
16 H. Furutani, H. Fukumura, H. Masuhara, S. Kambara, T. Kitaguchi, H. Tsukada, T. Ozawa: J. Phys. Chem. B **102**, 3395 (1998)
17 H. Furutani, H. Fukumura, H. Masuhara: Appl. Phys. Lett. **65**, 3413 (1994)
18 H. Furutani, H. Fukumura, H. Masuhara, T. Lippert, A. Yabe: J. Phys. Chem. A **101**, 5742 (1997)
19 R. Srinivasan: Appl. Phys. A **56**, 417 (1993)
20 L.S. Bennett, T. Lippert, H. Furutani, H. Fukumura, H. Masuhara: Appl. Phys. A **63**, 327 (1996)
21 J. Stebani, O. Nuyken, T. Lippert, A. Wokaun: Makromol. Chem. Rapid Commun. **206**, 2943 (1993)
22 D. Breitling, H. Schittenhelm, P. Berger, F. Dausinger, H. Hügel: Appl. Phys. A **69** 505 (1999)
23 M. Takeda, H. Ina, S. Kobayashi: J. Opt. Soc. **72**, 156 (1982)
24 K.T. Gahagan, D.S. Moore, D.J. Funk, J.H. Reho, R.L. Rabie: J. Appl. Phys. **92**, 3679 (2002)
25 S. Küper, J. Brannon, K. Brannon: Appl. Phys. A **56**, 43 (1993)
26 G. Gorodetsky, T.G. Kazyaka, R.L. Melcher, R. Srinivasan: Appl. Phys. Lett. **46**, 828 (1985)
27 I.W. Boyd, R.B. Jackman: *photochemical precessing of electronic materials* (Academic, London, 1992)
28 R. Srinivasan, B. Braren, R.W. Dreyfus: J. Appl. Phys. **61**, 372 (1987)
29 R. Srinivasan, B. Braren: J. Polym. Sci. **22**, 2601 (1984)
30 J.E. Andrew, P.E. Dyer, D. Foster, P.H. Key: Appl. Phys. Lett. **43**, 717 (1983)